

Bayesian Degradation Analysis With Inverse Gaussian Process Models Under Time-Varying Degradation Rates

Weiwen Peng, Yan-Feng Li, Yuan-Jian Yang, Jinhua Mi, and Hong-Zhong Huang, *Member, IEEE*

Abstract—Degradation observations of modern engineering systems, such as manufacturing systems, turbine engines, and high-speed trains, often demonstrate various patterns of time-varying degradation rates. General degradation process models are mainly introduced for constant degradation rates, which cannot be used for time-varying situations. Moreover, the issue of sparse degradation observations and the problem of evolving degradation observations both are practical challenges for the degradation analysis of modern engineering systems. In this paper, parametric inverse Gaussian process models are proposed to model degradation processes with constant, monotonic, and S-shaped degradation rates, where physical meaning of model parameters for time-varying degradation rates is highlighted. Random effects are incorporated into the degradation process models to model the unit-to-unit variability within product population. A general Bayesian framework is extended to deal with the degradation analysis of sparse degradation observations and evolving observations. An illustrative example derived from the reliability analysis of a heavy-duty machine tool's spindle system is presented, which is characterized as the degradation analysis of sparse degradation observations and evolving observations under time-varying degradation rates.

Index Terms—Bayesian reliability, degradation model, degradation rate, inverse Gaussian process, random effect.

NOMENCLATURE

IG	Inverse Gaussian.
PDF	Probability density function.
CDF	Cumulative distribution function.
MLE	Maximum likelihood estimation.
$Y(t)$	Degradation process.
$\Lambda(t)$	Mean function of an inverse Gaussian process.
λ	Scale parameter of an inverse Gaussian process.
$IG(\Lambda(t), \lambda\Lambda^2(t))$	Inverse Gaussian process.

Manuscript received September 1, 2014; revised February 15, 2015, January 22, 2016, and October 8, 2016; accepted November 26, 2016. Date of publication January 2, 2017; date of current version March 1, 2017. This work was supported in part by the NSAF under Grant U13301055, in part by the National Science and Technology Major Project of China under Grant 2014ZX04014-011, and in part by the Fundamental Research Funds for the Central Universities under Grant ZYGX2016KYQD119. Associate Editor: Q. Feng. (*Corresponding Author: Hong-Zhong Huang.*)

The authors are with the Center for System Reliability and Safety, University of Electronic Science and Technology of China, Chengdu 611731, China (e-mail: wwpeng@uestc.edu.cn; yanfengli@uestc.edu.cn; yuanjyang@hotmail.com; jinhua mi@126.com; hzhuang@uestc.edu.cn).

Color versions of one or more of the figures in this paper are available online at <http://ieeexplore.ieee.org>.

Digital Object Identifier 10.1109/TR.2016.2635149

$f(y(t))$	Probability density function of $Y(t)$ at time instant t .
$R(t)$	Reliability function under the degradation process $Y(t)$.
$\Phi(\bullet)$	Cumulative distribution of a standard s -normal distribution.
$r(t)$	Degradation rate function.
$g(\bullet \delta, \gamma)$	Probability density function of a gamma distribution.
θ	Vector of model parameters.
$\pi(\theta)$	Prior distribution of model parameter θ .
\mathbf{Y}	Matrix of degradation observations.
θ_i^R	Random effect parameter of the i th unit.
θ^H	Hyper-parameter in a random effect model.
$L(\mathbf{Y} \theta)$	Likelihood function of degradation observations \mathbf{Y} .
$p(\theta \mathbf{Y})$	Posterior distribution of model parameters.
θ	Posterior sample of model parameters.
Δy	Degradation increment of a degradation process $Y(t)$.

I. INTRODUCTION

NOWADAYS, companies of modern engineering systems, such as manufacturing systems, commercial airplanes, and high-speed trains, are under great pressures to deliver competitive products with high reliability. The reliability of these systems has become a critical issue both for the desire of high availability, and for the pursuit of high safety. Various degradation analysis methods are developed for product reliability analysis [1]–[3] and system health management [4], [5]. Generally, in the degradation analysis, an indicator is identified as the manifestation of some hidden or unobservable failure processes of a product. The product fails when this indicator reaches a predefined threshold [6]. Examples of indicators include vibration signal for bearings [7], oil debris for lubrication [8], crack length for gears [9], and fatigue damage for structures [10], [11]. In the degradation analysis of modern engineering systems, two typical situations are often encountered: 1) sparse degradation observations obtained for a product that can only be observed at intermittent discrete time points [12], and 2) evolving degradation observations generated for a product that is subject to a process of continual monitoring. A classic example of the degradation analysis with sparse degradation observations

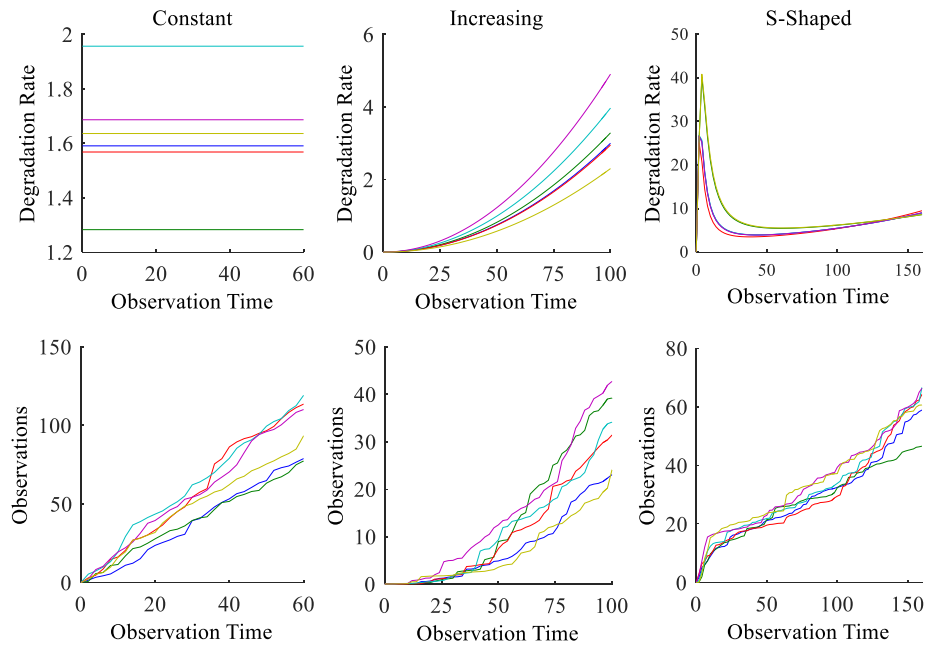


Fig. 1. Examples of constant, monotonic, and S-shaped degradation rates and relevant degradation observations.

and evolving observations, which motivates the study presented in this paper, is from the reliability analysis of a heavy-duty machine tool's spindle system. To ensure high productivity and low total cost of ownership, the machining accuracy, positioning accuracy, and oil debris of the spindle system can be monitored for the reliability analysis [13]–[15]. Due to the difference of measurement techniques, the positioning accuracy is measured sparsely during the spare time of machine tools, generating sparse degradation observations. However, the oil debris is monitored continually, generating evolving degradation observations.

To implement the degradation analysis, various degradation models are proposed to characterize different types of degradation observations [3], [16]. One type of degradation models is the degradation path model. Recent applications of degradation path models were presented for degradation analysis [17], [18], degradation test planning [19], [20], and system reliability modeling [21], [22]. Another type of degradation models is the stochastic-process-based degradation model. Recently, the gamma process models [23]–[25] and the Wiener process models [26]–[28] have been investigated extensively. However, the idea of degradation rate has not been highlighted and investigated thoroughly. To handle the situation with sparse or evolving degradation observations, a parametric description of the degradation rate is critical. This is out of the consideration that the degradation rate is an interpretation of a hidden failure mechanism of a product. It is also a direct description of the pattern of a degradation process, which can facilitate the empirical model selection by associating the failure mechanism with the degradation pattern. A pictorial description of degradation rates, including constant, increasing, and S-shaped degradation rates, and the relevant degradation processes is presented in Fig. 1.

In addition, another benefit to incorporate the parametric degradation rate is that subjective information integration and model updating can be implemented coherently. By specifying

probability distributions and updating the probability distributions for parameters of degradation models, subjective information integration for sparse degradation observations and model updating for evolving degradation observations can be implemented.

However, considering the degradation processes with monotonic increments, one challenge for the degradation models summarized above is the modeling of degradation processes with time-varying degradation rates. This is because the degradation path models with Gaussian measurement errors and degradation process models based on the Wiener process both have nonmonotonic increments. In addition, neither gamma process model nor nonparametric degradation model has analytical degradation rate for degradation modeling. Accordingly, the degradation analysis with time-varying degradation rates deserves further investigation.

In this paper, we propose a Bayesian method for the degradation analysis of degradation processes with constant, monotonic, and S-shaped degradation rates. These degradation models are proposed through the specification of parametric mean function of an IG process, which has been demonstrated as a flexible family for degradation modeling by Wang and Xu [29], Zhang *et al.* [30], Ye and Chen [31], Peng *et al.* [32], and Peng *et al.* [33]. A coherent Bayesian framework is constructed for the degradation analysis with the IG process models by extending the Bayesian framework introduced in our previous work [32]. Incorporation of subjective information for sparse degradation observations situation and updation of the degradation analysis for continual monitoring situation are handled within the Bayesian framework. We demonstrated the proposed method through the degradation analysis of a heavy-duty machine tool's spindle system. Model selection and comparison are studied in this illustrative example. The degradation analysis using the proposed IG process models is compared with the results obtained from the Wiener and gamma processes models.

The remainder of this paper is organized as follows. Section II introduces the IG process models for degradation modeling with constant, monotonic, and S-shaped degradation rates. Section III presents a general Bayesian framework for the degradation analysis with the IG process models. An illustrative example is then presented in Section IV to demonstrate the implementation of the Bayesian framework and the proposed IG process models for the degradation analysis. We then conclude the paper in Section V with remarks for future research.

II. IG PROCESS MODELS WITH CONSTANT, MONOTONIC, AND S-SHAPED DEGRADATION RATES

Assume the degradation process $\{Y(t), t \geq 0\}$ of a unit follows an IG process. $Y(t)$ has s -independent increments and $Y(t + \Delta t) - Y(t)$ follows an IG distribution as $IG(\Delta\Lambda, \lambda\Delta\Lambda^2)$ with $\Delta\Lambda = \Lambda(t + \Delta t) - \Lambda(t)$, $Y(0) \equiv 0$, and $\lambda > 0$ [31], [32]. Given a predefined failure threshold D for the degradation process $Y(t)$, the PDF of $Y(t)$ and the corresponding reliability function of the unit are separately given as

$$f(y(t) | \Lambda(t), \lambda) = \sqrt{\frac{\lambda\Lambda^2(t)}{2\pi y(t)^3}} \exp\left[-\frac{\lambda(y(t) - \Lambda(t))^2}{2y(t)}\right] \quad (1)$$

$$R(t | \Lambda(t), \lambda) = \Phi\left[\sqrt{\frac{\lambda}{D}}(D - \Lambda(t))\right] + \exp(2\lambda\Lambda(t)) \Phi\left[-\sqrt{\frac{\lambda}{D}}(D + \Lambda(t))\right]. \quad (2)$$

The degradation process of the unit is then described as $Y(t) \sim IG(\Lambda(t), \lambda\Lambda^2(t))$. It has a degradation mean given as $\Lambda(t)$ and a degradation variance given as $\Lambda(t)/\lambda$. In order to model the degradation process with constant, monotonic, and S-shaped degradation rates, parametric functions are introduced for the degradation mean function $\Lambda(t)$. The degradation rate function $r(t)$ is defined based on the degradation mean function as

$$r(t) = \frac{\partial\Lambda(t)}{\partial t}. \quad (3)$$

The degradation rate function is a quantitative description of the approximated slope or steepness of the degradation curve. A bigger value of $r(t)$ indicates a faster degradation rate, which means that a larger degradation increment $\Delta Y(t)$ is observed within a time interval Δt . In addition, the functional relationship between the degradation rate $r(t)$ and the observation time t is a description of the changing of the degradation process over time. Accordingly, based on the idea of incorporating parametric function of degradation rate, the IG process models for degradation processes with constant, monotonic, and S-shaped degradation rates are introduced.

A constant degradation rate $r_C(t)$ is corresponding to a degradation process with steady degradation velocity $\Lambda_C(t)$, such as the linear degradation curve in Fig. 1 (left). The degradation mean function with constant degradation rate is mathematically

modeled as

$$\Lambda_C(t) = \int r_C(t) dt = \mu t, \quad \mu > 0. \quad (4)$$

A monotonic degradation rate $r_M(t)$ is related to the degradation process for which the degradation velocity is gradually getting deteriorative (alleviative) for an increasing (decreasing) degradation rate, such as the one presented in Fig. 1 (middle). The degradation mean function with monotonic degradation rate is mathematically modeled as

$$\Lambda_M(t) = \int r_M(t) dt = \left(\frac{t}{\eta}\right)^\beta, \quad \beta > 0, \eta > 0. \quad (5)$$

The idea of this degradation rate function originates from the failure rate of a Weibull distribution [34]. The parameters β and η are separately shape parameter and scale parameter. The shape of the degradation rate depends on the parameter β : $0 < \beta < 1$ leads to a decreasing degradation rate; $\beta > 1$ leads to an increasing degradation rate; and $\beta = 1$ leads to a constant degradation rate, which equals to the IG process model introduced above with $r_C(t) = 1/\eta$.

An S-shaped degradation rate $r_S(t)$ is introduced for a complicated degradation process, which is presented in Fig. 1 (right). It describes a deteriorative process in the beginning, an alleviative process following on, a stable process for a relative long time, and finally, a deteriorative process until failure. The degradation mean function with the S-shaped degradation rate is mathematically modeled as

$$\Lambda_S(t) = \int r_S(t) dt = \nu \exp\left(\alpha \left(\frac{t}{\nu}\right) - \omega \left(\frac{t}{\nu}\right)^{-1}\right), \quad \begin{cases} \alpha > 0, \omega > 0, \\ \nu > 0. \end{cases} \quad (6)$$

The parameter α is a shape parameter of the degradation rate function. The degradation rate has an S-shaped curve when $0 < \alpha < 0.25$, and an increasing degradation rate when $\alpha \geq 0.25$. The parameters ω and ν are the scale parameters of the degradation rate function. The parameter ω adjusts the dispersion of the upside-down part of the S-shaped degradation rate function, which takes the value $0 < \omega < 1$ when an S-shaped degradation rate is introduced by the parameter. The parameter ν moderates the overall dispersion of the S-shaped degradation rate function.

By submitting the corresponding degradation mean functions given above into (1) and (2), the PDF and reliability function under the IG process degradation model with time-varying degradation rates can be obtained. When heterogeneous degradation rates within a population are considered, a common practice to incorporate random effect into the IG process model is to let a specific parameter with clear physical interpretation to vary randomly across units [31], [32]. For the degradation process models with constant, monotonic, and S-shaped degradation rates, practical ways to incorporate random effects are separately to let μ (rate parameter), η (scale parameter), and ν (scale parameter) follow a specific probability distribution. To demonstrate this idea, let the scale parameter ν of an S-shaped degradation rate follow a gamma distribution as $\nu \sim \text{Gamma}(\delta_\nu, \gamma_\nu)$. The

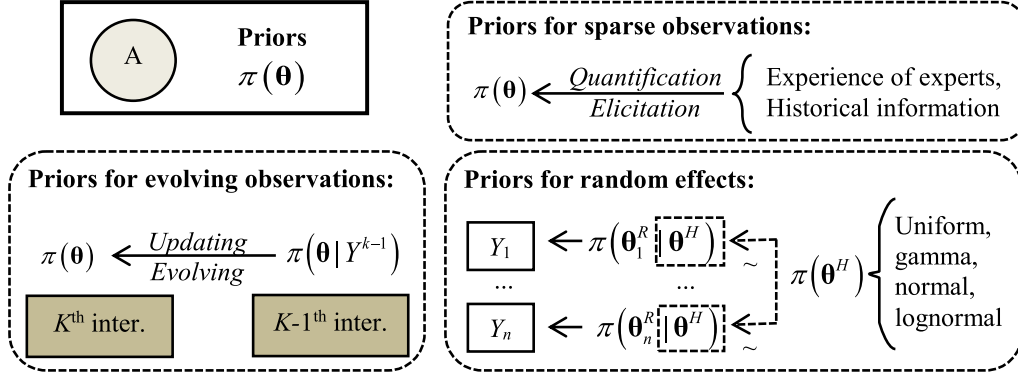


Fig. 2. General Bayesian framework for the IG process models: elicitation of prior distributions.

IG process model with S-shaped degradation rate and random effect is given as $Y_{SE}(t) \sim \text{IG}(\Lambda_S(t), \lambda_{SE}\Lambda_S(t)^2)$ with $\Lambda_S(t) = \nu \exp(\alpha(t/\nu) - \omega(t/\nu)^{-1})$ and $\nu \sim \text{Gamma}(\delta_\nu, \gamma_\nu)$. The PDF and reliability function of the S-shaped degradation model with random effect are given as

$$f_{SE}(y(t) | \alpha, \omega, \delta_\nu, \gamma_\nu, \lambda_{SE}) = \int_{\nu > 0} \left(f(y(t) | \Lambda_S(t), \lambda_{SE}) \times g_\nu(\nu | \delta_\nu, \gamma_\nu) \right) d\nu \quad (7)$$

$$R_{SE}(t | \alpha, \omega, \delta_\nu, \gamma_\nu, \lambda_{SE}) = \int_{\nu > 0} \left(R(t | \Lambda_S(t), \lambda_{SE}) \times g_\nu(\nu | \delta_\nu, \gamma_\nu) \right) d\nu. \quad (8)$$

III. GENERAL BAYESIAN FRAMEWORK FOR THE IG PROCESS MODELS

We extend the Bayesian framework presented in our previous work [32] in this section to handle the difficulties introduced by the situation with sparse degradation observations, and the situation with evolving observations. In detail, the method for prior derivation presented in [32] is extended and presented in Fig. 2. Three situations are considered for the prior derivation: the situation with sparse observations, the situation with evolving observations, and the situation with heterogeneous observations due to random effects, which are presented as separate blocks in Fig. 2. Different strategies can be chosen from the prior derivation methods based on the actual situation encountered.

For the situation with sparse degradation observations, one difficulty is that the observations cannot be readily analyzed to determine the parametric form of the underlying degradation model. To solve this problem, the strategies for subjective information quantification and multiple information fusion are used to facilitate the degradation analysis. As presented in Fig. 2, experts' experience and historical information are used to supplement the sparse degradation observations. Commonly, it is difficult to elicit experts' probabilities for model parameters of general degradation models, due to the lack of explicit physical interpretation of these model parameters [35]. However, this difficulty can be overcome by utilizing the idea of degradation rate and degradation mean functions. In detail, experts' experience and historical information are used to elicit probabilities on the degradation mean at a specific time point,

and on the shape parameter of a degradation function as well. Both of these parameters have explicit physical interpretation, such as the degradation mean is a description of the average degradation level at a specific time, and the shape parameter of a degradation function is related to the characteristics of the degradation process with constant, monotonic, or S-shaped degradation rate. Accordingly, subject information can be quantified with methods for expert elicitation [36] and prior derivation [37] based on these physical interpretations. Given the prior distributions for degradation mean and shape parameter, prior distributions for the remaining model parameters can then be obtained through multivariate transformation by utilizing the function relationship between the degradation mean function and model parameters. Take the IG process model with monotonic degradation rate as an example, which is given in (5). Experts' experience and historical information are first quantified into the probability distributions $\pi(\Lambda_M(t))$ and $\pi(\beta)$. The prior distribution for scale parameter of the IG process model with monotonic degradation rate can be obtained through the function relationship described by (5) as follows:

$$\pi(\eta) = \left\{ \eta : \eta = t(\Lambda_M(t))^{-1/\beta} \left| \begin{array}{l} \Lambda_M(t) \sim \pi(\Lambda_M(t)) \\ \beta \sim \pi(\beta) \end{array} \right. \right\}. \quad (9)$$

The probability distribution $\pi(\eta)$ can be obtained analytically or through simulation-based methods. For a simulation-based method, the procedure is given as follows:

- 1) generate samples from the probability distributions of $\pi(\Lambda_M(t))$ and $\pi(\beta)$,
- 2) obtain samples for parameter η based on the samples of $\pi(\Lambda_M(t))$ and $\pi(\beta)$ through the given function relationship, and
- 3) fit a suitable probability distribution to these samples to get $\pi(\eta)$.

For the situation with evolving degradation observations, the idea of model updating is used for prior derivation as presented in Fig. 2. The posterior distribution for the $K-1$ th degradation observations \mathbf{Y}^{K-1} is used as the prior distribution for the K th degradation observations. The estimation results obtained from the $K-1$ th degradation observations are then updated coherently by incorporating the information of the K th degradation observations without reanalyzing $K-1$ th degradation observations. In practical application, it is often difficult to obtain an analytical form of the posterior distribution for the $K-1$ th degradation ob-

servations \mathbf{Y}^{K-1} , which causes difficulty for directly using this posterior distribution as priors for the K^{th} degradation observations. To solve this problem, posterior samples are obtained from the $K-1^{\text{th}}$ degradation observations through Markov chain Monte Carlo simulation (MCMC), and these posterior samples are further fitted to specific probability distributions. These fitted probability distributions are used as prior distributions in the following degradation analysis of the K^{th} degradation observations.

In addition, the method of hierarchical priors is used for the degradation analysis with random effects. Let θ_i^R with $i = 1, \dots, n$ denote the random effect parameter within a population group with sample size n , and θ^H denote the hyper-parameter, which is the parameter of the probability distribution of the θ_i^R . Take the IG process model with S-shaped degradation rate and random effect as an example, which is given as $Y_{SE}(t) \sim \text{IG}(\Lambda_{S,i}(t), \lambda_{SE} \Lambda_{S,i}(t)^2)$ with $\Lambda_{S,i}(t) = \nu_i \exp(\alpha(t/\nu_i) - \omega(t/\nu_i)^{-1})$ and $\nu_i \sim \text{Gamma}(\delta_\nu, \gamma_\nu)$, the random effect parameter θ_i^R includes ν_i , and the hyper-parameter θ^H includes δ_ν and γ_ν . Furthermore, let $\pi(\theta_i^R | \theta^H)$ denote the prior distribution for the random effect parameter θ_i^R , which is unique for the i^{th} individual sample. $\pi(\theta^H)$ is the prior distribution for the hyper-parameter, which is the same for all the prior distributions $\pi(\theta_i^R | \theta^H)$ with $i = 1, \dots, n$. The connection among individual samples within the product population is constructed by the prior distribution of hyper-parameter $\pi(\theta^H)$. As a result, random effect information within the product population is integrated through these hierarchical prior distributions. To derive the hierarchical priors in practical applications, subjective information is used to choose a probability distribution to characterize the individuality of the random effect parameter. The probability distributions often used for random effect parameter within the IG process degradation model include the truncated normal distribution, gamma distribution, and log-normal distribution [31], [32]. In addition, the method of prior derivation described above for sparse degradation observations can be used to obtain priors for random effect parameters with clear physical meanings. For the hyper-parameters, diffuse priors such as uniform distributions with large intervals and gamma distribution with large variance are often used. This is due to the consideration that there is no direct physical meaning of the hyper-parameters, and it is impractical to directly quantify prior information into the hyper-parameters.

IV. ILLUSTRATIVE EXAMPLE: RELIABILITY ANALYSIS OF A HEAVY-DUTY MACHINE TOOL'S SPINDLE SYSTEM

The spindle system of a heavy-duty machine tool transmits the required energy and rotates the tool precisely to implement high-precision machining processes, such as grinding, milling, and drilling. It has a significant impact on the material removal rate and the final quality of machined parts [38]. The spindle system of a machine tool is consequently expected to demonstrate high reliability and availability. Tense condition monitoring and health management are implemented on the spindle system. The bearings, ball screw, and gears are generally responsible for the failures of the spindle system. The monitoring of the machining accuracy, positioning accuracy, and the amount of debris in the

TABLE I
DEGRADATION OBSERVATIONS OF POSITIONING ACCURACY

Sample 1	Time	26	28	32	46	78	88	92	154	180
	Observations	70	72	77	101	157	196	205	312	362
Sample 2	Time	18	22	44	52	70	118	132	160	180
	Observations	4	8	20	32	49	71	75	99	115
Sample 3	Time	26	28	50	86	106	128	134	138	178
	Observations	38	39	97	165	223	273	277	284	375
Sample 4	Time	22	40	42	44	66	110	160	162	174
	Observations	25	36	38	39	56	91	153	153	168
Sample 5	Time	44	64	92	94	110	114	120	124	148
	Observations	43	75	110	116	142	144	155	164	189

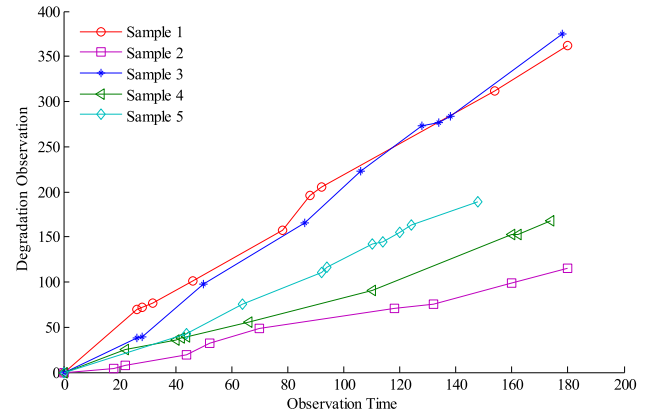


Fig. 3. Degradation observations of positioning accuracy.

lubricant oil (oil debris) are used to track the deterioration of these units. In this section, the IG process models introduced above are implemented to the degradation analysis of the spindle system using the proposed Bayesian framework.

To avoid proprietary issues, the units of values are omitted, and the data are modified in a certain way. Largely, however, the characteristics of the degradation observations, and the application of the proposed IG process degradation models and the Bayesian method are the same as the original.

A. Degradation Analysis of Positioning Accuracy: IG Process Model With Constant Degradation Rate and Random Effects

Five spindle systems have been measured in a period of six months. Due to the limitation of cost and measuring technique, the measurements of positioning accuracy of these spindle system are implemented discretely. As a result, a group of sparse degradation observations are observed, and presented in Table I and Fig. 3.

Let $Y_{CE}(t_{ij})$ with $j = 1, \dots, m_i$ and $i = 1, \dots, 5$ be the j^{th} observation for sample i at observation time t_{ij} , where m_i is the number of observations of the i^{th} sample. Let $\Delta y_{ij}^{\text{CE}} = Y_{CE}(t_{ij}) - Y_{CE}(t_{i,j-1})$ be the degradation increment. Then, under the IG process degradation model with constant degradation rate and random effect, $\Delta y_{ij}^{\text{CE}}$ are independent and follow IG distribution $\text{IG}(\Delta \Lambda_{ij}^{\text{CE}}, \lambda_{\text{CE}} (\Delta \Lambda_{ij}^{\text{CE}})^2)$ with $\Delta \Lambda_{ij}^{\text{CE}} = \mu_i t_{ij} - \mu_i t_{i,j-1}$ and $\mu_i \sim \text{Gamma}(\delta_\mu, \gamma_\mu)$.

Following the framework presented in Fig. 2, experts' experience and historical information are used to derive probability

distribution of the degradation mean μt and degradation variance $\mu t/\lambda$ at a serial of observation points. Similar to the transformations of random variables presented in (9), these derived distributions are transformed to the prior distributions of model parameters $\boldsymbol{\theta} = \{\delta_\mu, \gamma_\mu, \lambda_{\text{CE}}\}$ as

$$\begin{cases} \delta_\mu \sim \text{Gamma}(20, 2), \gamma_\mu \sim \text{Gamma}(15, 1.5), \\ \lambda_{\text{CE}} \sim \text{Lognormal}(0.3, 0.3^2) \end{cases} \quad (10)$$

where $\text{Lognormal}(0.3, 0.3^2)$ is a log-normal distribution.

The likelihood function for the degradation observations of positioning accuracy is given as (11) at the bottom of the page, where $\boldsymbol{\mu} = (\mu_1, \dots, \mu_5)$.

Based on the prior distributions and the likelihood function, the Bayesian estimation of model parameters, which is the joint posterior distribution of model parameters, is obtained as (12) at the bottom of the page.

The MCMC method is used to simulate samples of model parameters from the joint posterior distribution in (12). For the degradation analysis of positioning accuracy, 20 000 samples are generated using the OpenBUGS [39]. Parameter estimation, degradation inference, reliability assessment, and residual life prediction are implemented based on the generated samples of posterior distribution.

The degradation inferences for individual sample and the population are obtained based on the joint posterior distribution of model parameters as shown in (13) and (14) at the bottom of the page, where $f_C(y_{i,m+k}|\mathbf{Y}_{\text{CE}})$ is the PDF of the degradation of

the i th sample at future time point $t_{i,m+k}$, and $f_{\text{CE}}(y_{\text{CE}}|\mathbf{Y}_{\text{CE}})$ is the PDF of the degradation of the population at time point t .

The calculations of (13) and (14) are implemented using Monte Carlo integration based on the posterior samples generated above. For the degradation inference at a specific time point, 20 000 samples of degradation inference are obtained based on the 20 000 posterior samples of related model parameters. The statistics of this degradation inference, such as the mean, variance, and quantiles, are then obtained based on its posterior samples. In detail, the degradation inference for the i th degradation curve is based on the samples $\tilde{\boldsymbol{\theta}} = \{\tilde{\mu}_i, \tilde{\lambda}_{\text{CE}}\}$ from $p(\mu_i, \lambda_{\text{CE}}|\mathbf{Y}_{\text{CE}})$, and the IG distribution $\text{IG}(\Delta\tilde{\Lambda}_{ij}^{\text{CE}}, \tilde{\lambda}_{\text{CE}}(\Delta\tilde{\Lambda}_{ij}^{\text{CE}})^2)$ with $\Delta\tilde{\Lambda}_{ij}^{\text{CE}} = \tilde{\mu}_i t_{ij} - \tilde{\mu}_i t_{i,j-1}$. The degradation inference for the population is based on the samples $\tilde{\boldsymbol{\theta}} = \{\tilde{\delta}_\mu, \tilde{\gamma}_\mu, \tilde{\lambda}_{\text{CE}}\}$ from $p(\delta_\mu, \gamma_\mu, \lambda_{\text{CE}}|\mathbf{Y}_{\text{CE}})$, and the IG distribution $\text{IG}(\Delta\tilde{\Lambda}_j^{\text{CE}}, \tilde{\lambda}_{\text{CE}}(\Delta\tilde{\Lambda}_j^{\text{CE}})^2)$ with $\Delta\tilde{\Lambda}_j^{\text{CE}} = \tilde{\mu} t_j - \tilde{\mu} t_{j-1}$ and $\tilde{\mu} \sim \text{Gamma}(\tilde{\delta}_\mu, \tilde{\gamma}_\mu)$.

For the degradation of positioning accuracy, there are ten degradation observations for each sample. The first seven observations are used to estimate model parameters. The remaining three observations are retained as cross-validation observations. To test the precision of degradation inference, the error of the degradation inference is defined as

$$\text{error} = \frac{|\text{inferred degradation} - \text{observed degradation}|}{\text{observed degradation}}. \quad (15)$$

Based on the 20 000 posterior samples of model parameter, a group of 20 000 samples of degradation inferences and the

$$\begin{aligned} L(\mathbf{Y}_{\text{CE}}, \boldsymbol{\mu}|\delta_\mu, \gamma_\mu, \lambda_{\text{CE}}) &= \prod_{i=1}^5 g_\mu(\mu_i|\delta_\mu, \gamma_\mu) \prod_{j=2}^{m_i} f(\Delta y_{ij}^{\text{CE}}|\Delta\Lambda_{ij}^{\text{CE}}, \lambda_{\text{CE}}) \\ &= \prod_{i=1}^5 \frac{\gamma_\mu^\delta \mu_i^{\delta-1}}{\Gamma(\delta_\mu)} \exp(-\gamma_\mu \mu_i) \prod_{j=2}^{m_i} \sqrt{\frac{\lambda_{\text{CE}} (\Delta\Lambda_{ij}^{\text{CE}})^2}{2\pi (\Delta y_{ij}^{\text{CE}})^3}} \exp\left[-\frac{\lambda_{\text{CE}} (\Delta y_{ij}^{\text{CE}} - \Delta\Lambda_{ij}^{\text{CE}})^2}{2\Delta y_{ij}^{\text{CE}}}\right] \end{aligned} \quad (11)$$

$$p(\boldsymbol{\mu}, \delta_\mu, \gamma_\mu, \lambda_{\text{CE}}|\mathbf{Y}_{\text{CE}}) \propto \pi(\delta_\mu, \gamma_\mu, \lambda_{\text{CE}}) L(\mathbf{Y}_{\text{CE}}, \boldsymbol{\mu}|\delta_\mu, \gamma_\mu, \lambda_{\text{CE}})$$

$$\begin{aligned} &\propto \delta_\mu^{20-1} \exp(-2\delta_\mu) \gamma_\mu^{15-1} \exp(-1.5\gamma_\mu) \lambda_{\text{CE}}^{-1} \exp\left(-\frac{(\ln \lambda_{\text{CE}} - 0.3)^2}{2 \times 0.3^2}\right) \\ &\quad \times \prod_{i=1}^5 \left\{ \frac{\gamma_\mu^\delta \mu_i^{\delta-1}}{\Gamma(\delta_\mu)} \exp(-\gamma_\mu \mu_i) \prod_{j=2}^{m_i} \sqrt{\frac{\lambda_{\text{CE}} (\Delta\Lambda_{ij}^{\text{CE}})^2}{2\pi (\Delta y_{ij}^{\text{CE}})^3}} \exp\left[-\frac{\lambda_{\text{CE}} (\Delta y_{ij}^{\text{CE}} - \Delta\Lambda_{ij}^{\text{CE}})^2}{2\Delta y_{ij}^{\text{CE}}}\right] \right\} \end{aligned} \quad (12)$$

$$f_C(y_{i,m+k}|\mathbf{Y}_{\text{CE}}) = \int_{\mu_i, \lambda_{\text{CE}}} f(y_{i,m+k}|\Lambda_C(t_{i,m+k}), \lambda_{\text{CE}}) p(\mu_i, \lambda_{\text{CE}}|\mathbf{Y}_{\text{CE}}) d\mu_i d\lambda_{\text{CE}} \quad (13)$$

$$f_{\text{CE}}(y_{\text{CE}}|\mathbf{Y}_{\text{CE}}) = \int_{\delta_\mu, \gamma_\mu, \lambda_{\text{CE}}} \int_{\mu_i > 0} f(y_{\text{CE}}|\Lambda_C(t), \lambda_{\text{CE}}) g_\mu(\mu_i|\delta_\mu, \gamma_\mu) d\mu_i \times p(\delta_\mu, \gamma_\mu, \lambda_{\text{CE}}|\mathbf{Y}_{\text{CE}}) d\delta_\mu d\gamma_\mu d\lambda_{\text{CE}} \quad (14)$$

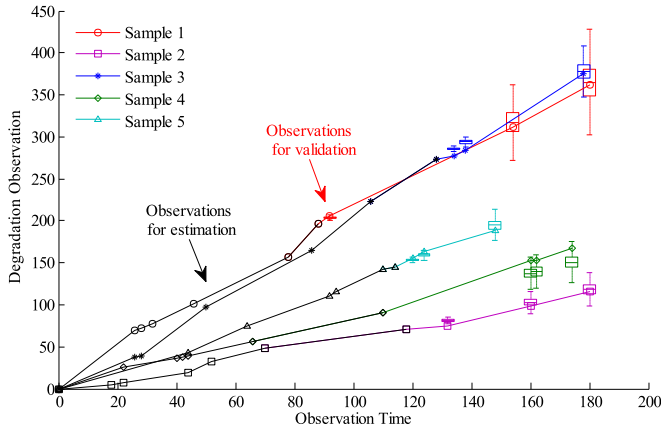


Fig. 4. Degradation inferences of positioning accuracy.

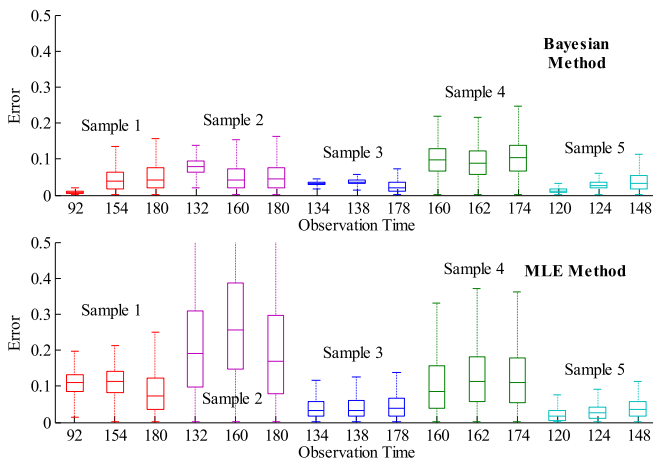


Fig. 5. Errors of degradation inferences by the Bayesian method and the MLE method.

corresponding errors are obtained for each cross-validation observation. The statistics of the samples of degradation inferences and errors are summarized, and presented in Figs. 4 and 5. For the boxplots, the central mark is the median of the error, the edges of the box are the 25th and the 75th percentiles of the error, and the whiskers extend to the most extreme errors not considered as outliers. Both the boxplots of the degradation inferences and the inference errors demonstrate that the proposed method has a high precision.

To further demonstrate the capability of the Bayesian method for the degradation analysis with sparse degradation observations, a comparison of the proposed Bayesian method and the non-Bayesian method is studied. The errors of degradation inferences for the validation observations are given in Fig. 5, which are separately generated by the proposed Bayesian method and the MLE method. A higher precision is obtained by the proposed Bayesian method with informative priors over the MLE. This is mainly due to the incorporation of prior information through the Bayesian method introduced above, which is critical for the degradation analysis of sparse degradation observations. However, the incorporation of prior information cannot be implemented based on the MLE. The capability of the proposed

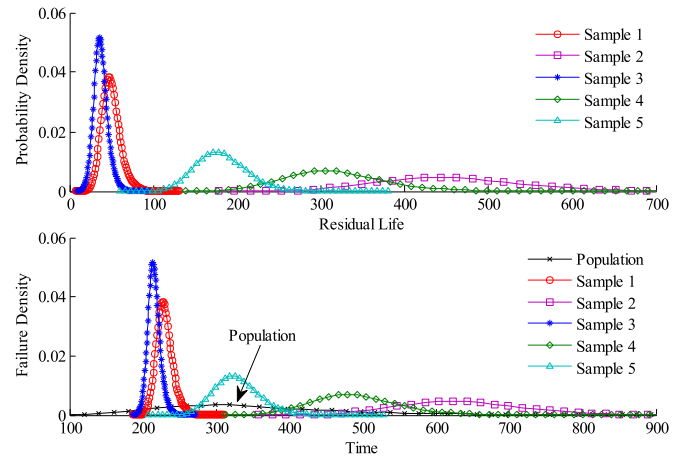


Fig. 6. Residual life prediction for individual samples (upper), and failure density function of individual samples and the population of the ball crews (lower).

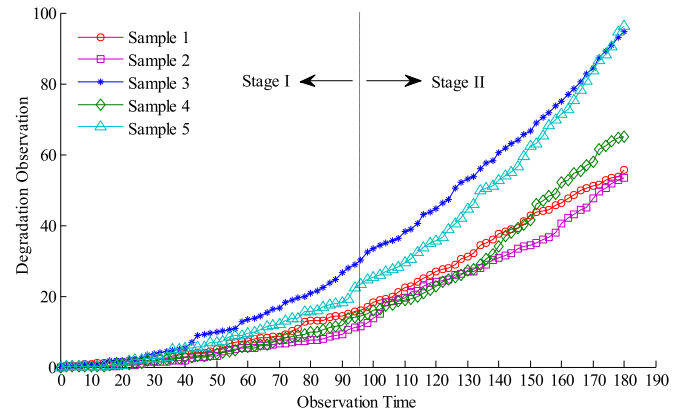


Fig. 7. Degradation observations of amount of oil debris.

method for the degradation analysis with sparse degradation observations is demonstrated.

Given the threshold of the degradation process as $D_{CE} = 450$, residual life for each individual sample and the reliability of the population are obtained and given in Fig. 6.

B. Degradation Analysis of Oil Debris: IG Process Model With Increasing Degradation Rate and Random Effects

The gradual increase of amount of oil debris is related to the degradation process of gears. Metallic wear debris sensors are embedded in the lubricating systems of the five spindle systems. Continual monitoring of the amount of oil debris is implemented. Degradation observations are presented in Fig. 7. The degradation analysis is divided into two separate stages, i.e., stage I and stage II in Fig. 7, to demonstrate the proposed Bayesian method for the situation of evolving degradation observations.

An increasing degradation rate is chosen for the degradation process of the amount of oil debris. It is mainly based on the experience of experts in that domain, and the overall trend of the degradation curve presented in Fig. 7. In addition,

heterogeneity is presented among the degradation curves. The IG process model with a monotonic degradation rate and random effect is consequently used to model the degradation process. The degradation increment of oil debris $\Delta y_{ij}^{\text{ME}} = Y_{\text{ME}}(t_{ij}) - Y_{\text{ME}}(t_{i,j-1})$ is model as $\text{IG}(\Delta\Lambda_{ij}^{\text{ME}}, \lambda_{\text{ME}}(\Delta\Lambda_{ij}^{\text{ME}})^2)$ with $\Delta\Lambda_{ij}^{\text{ME}} = (t_{ij}/\eta_i)^{\beta_i} - (t_{i,j-1}/\eta_i)^{\beta_i}$ and $\eta_i \sim \text{Gamma}(\delta_\eta, \gamma_\eta)$.

Compared with the degradation analysis of positioning accuracy, the information contained in the degradation observations of oil debris is sufficient for parameter estimations. To simplify the Bayesian degradation analysis, we used the noninformative prior distributions for the degradation analysis in stage I as follows:

$$\begin{cases} \delta_\eta \sim \text{Uniform}(0, 100), \gamma_\eta \sim \text{Uniform}(0, 100), \\ \beta \sim \text{Uniform}(0, 10), \lambda_{\text{ME}} \sim \text{Uniform}(0, 100). \end{cases} \quad (16)$$

The likelihood function for the degradation observations of oil debris is given as shown in (17) at the bottom of the page, where $\boldsymbol{\eta} = (\eta_1, \dots, \eta_5)$.

The joint posterior distribution of model parameters in stage I is obtained as follows:

$$\begin{aligned} p_I(\boldsymbol{\eta}, \delta_\eta, \gamma_\eta, \beta, \lambda_{\text{ME}} | \mathbf{Y}_{\text{ME}}^{\text{I}}) &\propto \pi_I(\delta_\eta, \gamma_\eta, \beta, \lambda_{\text{ME}}) \\ &\times L_I(\mathbf{Y}_{\text{ME}}^{\text{I}}, \boldsymbol{\eta}, |\delta_\eta, \gamma_\eta, \beta, \lambda_{\text{ME}}). \end{aligned} \quad (18)$$

When the degradation observations of stage II are available, the joint posterior distribution of model parameters in stage I is used as the prior distribution in the degradation analysis in stage II. The joint posterior distribution for model parameters in stage II is obtained as

$$\begin{aligned} p_{\text{II}}(\boldsymbol{\eta}, \delta_\eta, \gamma_\eta, \beta, \lambda_{\text{ME}} | \mathbf{Y}_{\text{ME}}) &\propto p_I(\delta_\eta, \gamma_\eta, \beta, \lambda_{\text{ME}} | \mathbf{Y}_{\text{ME}}^{\text{I}}) \\ &\times L_{\text{II}}(\mathbf{Y}_{\text{ME}}^{\text{II}}, \boldsymbol{\eta}, |\delta_\eta, \gamma_\eta, \beta, \lambda_{\text{ME}}) \end{aligned} \quad (19)$$

where $p_I(\delta_\eta, \gamma_\eta, \beta, \lambda_{\text{ME}} | \mathbf{Y}_{\text{ME}}^{\text{I}})$ is the joint posterior distribution given in (18). $L_{\text{II}}(\mathbf{Y}_{\text{ME}}^{\text{II}}, \boldsymbol{\eta}, |\delta_\eta, \gamma_\eta, \beta, \lambda_{\text{ME}})$ is the same as (17) with $\Delta y_{ij}^{\text{ME}}$ substituted by the degradation increments in stage II.

Based on the joint posterior distributions obtained in stage I and stage II, the degradation inference for individual samples $f_M(y_{i,m+k} | \mathbf{Y}_{\text{ME}})$ and the population $f_{\text{ME}}(y_{\text{ME}} | \mathbf{Y}_{\text{ME}})$ are obtained as shown in (20) and (21) on the bottom of the next page.

Similar to the degradation inferences for positioning accuracy, 20 000 samples are simulated from the joint posterior distributions for stage I and stage II using the OpenBUGS. The degradation inferences, residual life prediction for individual samples, and reliability assessment for the population are ob-

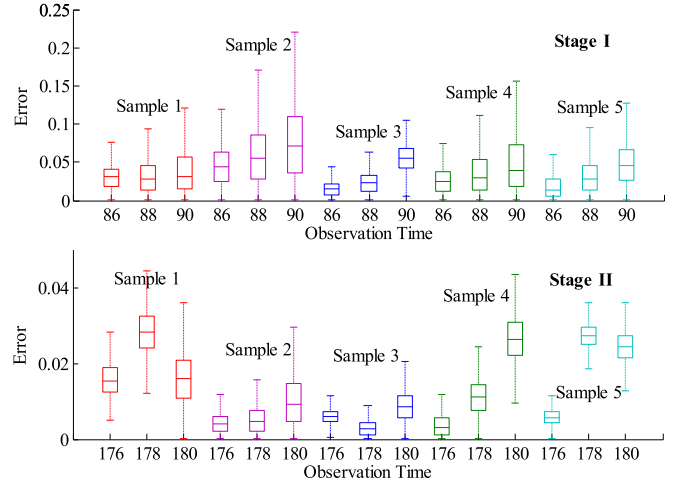


Fig. 8. Errors of degradation inferences in stage I and stage II.

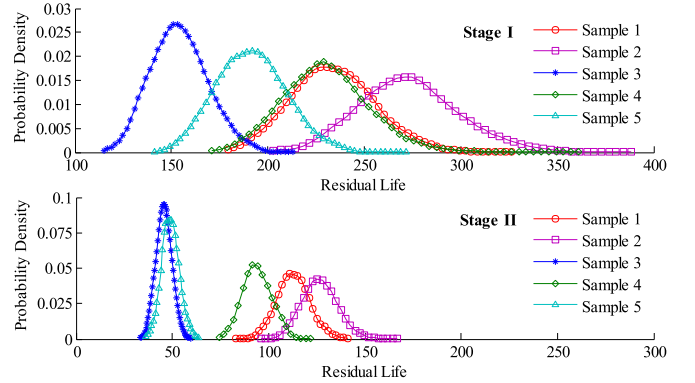


Fig. 9. Residual life prediction for individual gears in stage I and stage II.

tained through the simulation-based posterior analysis. Three degradation observations are reserved as validation observations. The errors of degradation inference for individual samples in stage I and stage II are presented in Fig. 8. It is shown in Fig. 8 that the precision of degradation inference improves a lot from stage I to stage II, which is due to the incorporation of posterior distribution in stage I as prior distribution for the degradation analysis in stage II.

The degradation threshold of the oil debris is $D_{\text{ME}} = 150$. The residual life predictions for individual samples and the reliability assessment for individual samples and the population in stage I and stage II are presented in Figs. 9 and 10.

The improvement of prediction precision from stage I to stage II is significant. This is ascribed to the effectiveness

$$\begin{aligned} L(\mathbf{Y}_{\text{ME}}, \boldsymbol{\eta}, |\delta_\eta, \gamma_\eta, \beta, \lambda_{\text{ME}}) &= \prod_{i=1}^5 g_\eta(\eta_i | \delta_\eta, \gamma_\eta) \prod_{j=2}^{m_i} f(\Delta y_{ij}^{\text{ME}} | \Delta\Lambda_{ij}^{\text{ME}}, \lambda_{\text{ME}}) \\ &= \prod_{i=1}^5 \frac{\gamma_\eta \eta_i^{\delta_\eta - 1}}{\Gamma(\delta_\eta)} \exp(-\gamma_\eta \eta_i) \prod_{j=2}^{m_i} \sqrt{\frac{\lambda_{\text{ME}} (\Delta\Lambda_{ij}^{\text{ME}})^2}{2\pi (\Delta y_{ij}^{\text{ME}})^3}} \exp\left[-\frac{\lambda_{\text{ME}} (\Delta y_{ij}^{\text{ME}} - \Delta\Lambda_{ij}^{\text{ME}})^2}{2\Delta y_{ij}^{\text{ME}}}\right] \end{aligned} \quad (17)$$

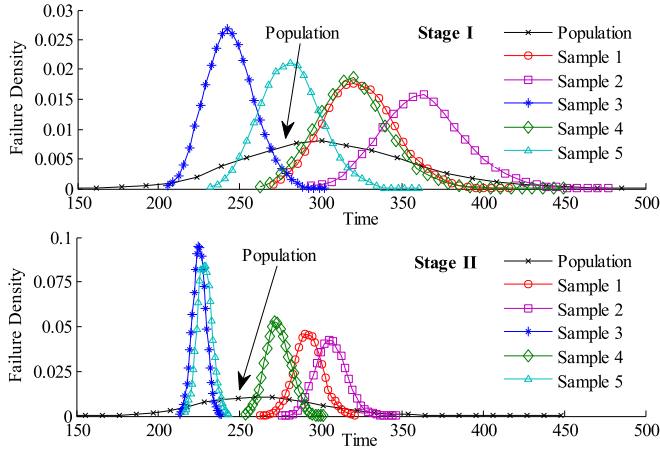


Fig. 10. Failure density function for individual gears and the population in stage I and stage II.

of the proposed Bayesian method for dealing with evolving degradation observations, where the posterior distribution in stage I is used as the prior distribution for the degradation analysis in stage II. The information in stage I is integrated with the information in stage II. The precision of the residual life prediction and reliability assessment is improved through this information integration. From this comparison of results between the stage I and stage II, the effectiveness of the proposed Bayesian method for the degradation analysis with evolving degradation observations is demonstrated.

C. Degradation Analysis of Machining Accuracy: IG Process Model With S-Shaped Degradation Rate and Random Effects

To obtain information about deterioration of bearings in the spindle systems, machining accuracy of five spindle systems is monitored. The machining accuracy is measured discretely during spare time of the machine tools. The degradation observations are presented in Table II and Fig. 11.

The IG process degradation model with S-shaped degradation rate is chosen for the degradation analysis of machining accuracy. It is mainly based on subjective experience of experts and historical information from similar machine tools. The degradation increment of machining accuracy $\Delta y_{ij}^{SE} = Y_{SE}(t_{ij}) - Y_{SE}(t_{i,j-1})$ is consequently model as $IG(\Delta\Lambda_{ij}^{SE}, \lambda_{SE}(\Delta\Lambda_{ij}^{SE})^2)$ with $\Delta\Lambda_{ij}^{SE} = \Lambda_S(t_{ij}) - \Lambda_S(t_{i,j-1})$ and $\nu_i \sim \text{Gamma}(\delta_\nu, \gamma_\nu)$. The degradation mean function $\Lambda_S(t)$ is given in (6).

Uniform distributions for model parameter $\theta = \{\alpha, \omega, \delta_\nu, \gamma_\nu, \lambda_{SE}\}$ are used as priors for the degradation analysis of

TABLE II
DEGRADATION OBSERVATIONS OF POSITIONING ACCURACY

Sample 1	Time	14	46	88	94	96	120	124	150	192	234
	Observations	8	17	23	23	23	25	25	29	43	52
	Time	244	258	262	288	308	324	334	364	408	
	Observations	52	54	55	59	65	72	75	84	98	
Sample 2	Time	4	6	26	32	58	70	148	158	208	214
	Observations	3	4	18	19	22	23	32	32	43	44
	Time	220	250	266	306	344	408	434	456	492	
	Observations	45	48	52	59	72	96	108	116	135	
Sample 3	Time	4	36	50	98	136	184	190	208	230	232
	Observations	2	15	16	19	25	29	30	31	35	35
	Time	256	276	300	302	306	324	334	398	442	
	Observations	41	44	46	47	47	53	55	72	81	
Sample 4	Time	60	62	96	98	128	136	162	216	288	304
	Observations	21	21	25	25	27	28	30	43	58	60
	Time	318	356	396	426	440	450	478	480	496	
	Observations	63	76	93	113	123	126	141	142	155	
Sample 5	Time	4	68	114	116	122	138	228	242	254	270
	Observations	0.01	15	19	19	20	21	31	32	32	35
	Time	334	382	402	406	422	424	426	442	458	
	Observations	44	54	55	55	56	56	57	59	61	

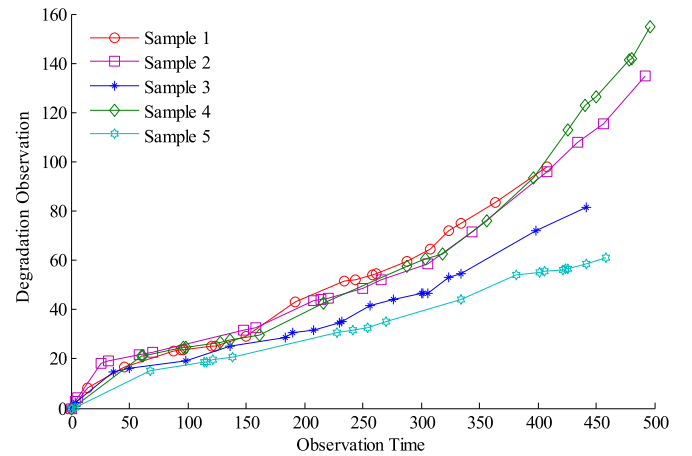


Fig. 11. Degradation observations of machining accuracy.

the machining accuracy as follows:

$$\begin{cases} \alpha \sim \text{Uniform}(0, 0.25), \omega \sim \text{Uniform}(0, 1), \\ \delta_\nu \sim \text{Uniform}(0, 100), \gamma_\nu \sim \text{Uniform}(0, 100), \\ \lambda_{SE} \sim \text{Uniform}(0, 100) \end{cases} \quad (22)$$

where the intervals of shape parameter α and scale parameter ω are bounded in the intervals for an S-shaped degradation rate. The remaining parameters are ascribed noninformative priors in the form of uniform distributions with large intervals.

$$f_M(y_{i,m+k} | \mathbf{Y}_{ME}) = \int_{\beta, \eta_i, \lambda_{ME}} f(y_{i,m+k} | \Lambda_M(t_{i,m+k}), \lambda_{ME}) p(\beta, \eta_i, \lambda_{ME} | \mathbf{Y}_{ME}) d\beta d\eta_i d\lambda_{ME} \quad (20)$$

$$f_{ME}(y_{ME} | \mathbf{Y}_{ME}) = \int_{\delta_\eta, \gamma_\eta, \beta, \lambda_{ME}} \int_{\eta_i > 0} f(y_{ME} | \Lambda_M(t), \lambda_{ME}) g_\eta(\eta_i | \delta_\eta, \gamma_\eta) d\eta_i \times p(\delta_\eta, \gamma_\eta, \beta, \lambda_{ME} | \mathbf{Y}_{ME}) d\delta_\eta d\gamma_\eta d\beta d\lambda_{ME} \quad (21)$$

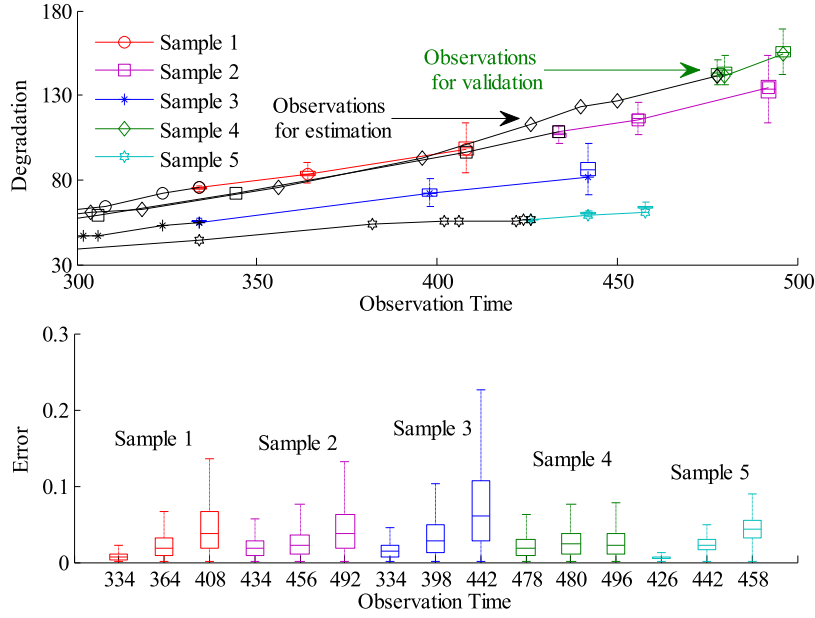


Fig. 12. Degradation inferences of machining accuracy (upper) and the inference errors (lower).

The likelihood function for the observations of machining accuracy is given as shown in (23) at the bottom of the page, where $\mathbf{v} = (\nu_1, \dots, \nu_5)$.

The joint posterior distribution of model parameters is obtained as follows:

$$p(\mathbf{v}, \alpha, \omega, \delta_\nu, \gamma_\nu, \lambda_{SE} | \mathbf{Y}_{SE}) \propto \pi(\alpha, \omega, \delta_\nu, \gamma_\nu, \lambda_{SE}) \times L(\mathbf{Y}_{SE}, \mathbf{v} | \alpha, \omega, \delta_\nu, \gamma_\nu, \lambda_{SE}). \quad (24)$$

The posterior samples are generated from (24). Similar to the posterior analysis of oil debris, the degradation inferences for individual samples and the corresponding errors are obtained and presented in Fig. 12. The degradation threshold of the machining accuracy is $D_{SE} = 300$. The residual life predictions for individual samples and the reliability assessment for the population are obtained and presented in Fig. 13.

D. Discussion on Model Selection and Comparison

Because three IG process models are introduced in this paper, model selection becomes a critical issue for the implementation of these models for the degradation analysis. One practical way is to combine the subjective testimony about the degradation rate with the qualitative analysis of the degradation curves. Due to the proposed IG process, degradation models are defined

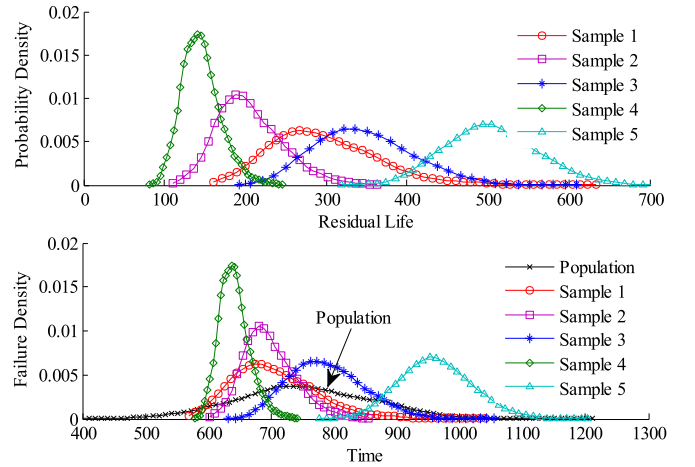


Fig. 13. Residual life prediction for individual samples (upper), and failure density function for individual samples and population of the bearings (lower).

for different degradation rates, experts' testimony can help to identify the specific type of degradation rate and to choose the right model. Other than the qualitative method for model selection, quantitative methods can also be introduced. The minimum Akaike information criterion (AIC) and the leave-out cross validation are two common ways for model selection and com-

$$L(\mathbf{Y}_{SE}, \mathbf{v} | \alpha, \omega, \delta_\nu, \gamma_\nu, \lambda_{SE}) = \prod_{i=1}^5 g_\nu(\nu_i | \delta_\nu, \gamma_\nu) \prod_{j=2}^{m_i} f(\Delta y_{ij}^{SE} | \Delta \Lambda_{ij}^{SE}, \lambda_{SE}) \\ = \prod_{i=1}^5 \frac{\gamma_\nu^{\delta_\nu} \nu_i^{\delta_\nu - 1}}{\Gamma(\delta_\nu)} \exp(-\gamma_\nu \nu_i) \prod_{j=2}^{m_i} \sqrt{\frac{\lambda_{SE} (\Delta \Lambda_{ij}^{SE})^2}{2\pi (\Delta y_{ij}^{SE})^3}} \exp\left[-\frac{\lambda_{SE} (\Delta y_{ij}^{SE} - \Delta \Lambda_{ij}^{SE})^2}{2\Delta y_{ij}^{SE}}\right] \quad (23)$$

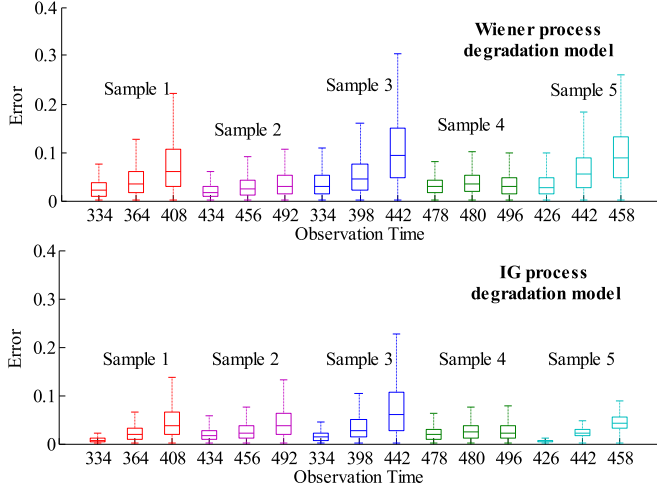


Fig. 14. Comparison of degradation inference errors between the Wiener process and IG process models.

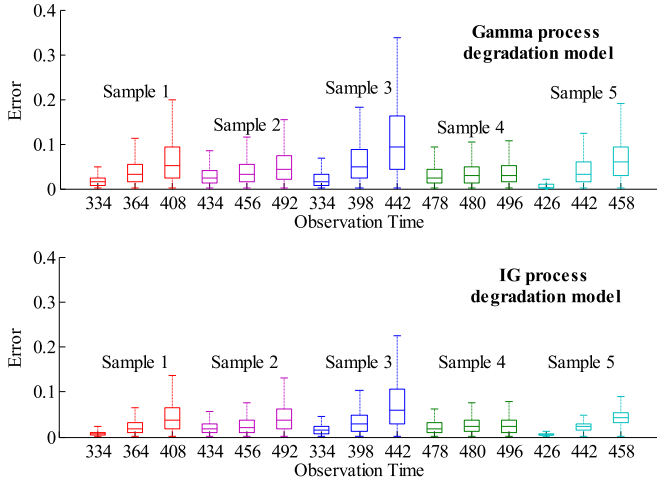


Fig. 15. Comparison of degradation inference errors between the gamma process and IG process models.

parison. The AIC value is defined as $AIC = 2k - 2l(\hat{\theta})$, where $k = |\theta|$ is the number of parameters in that model and $l(\hat{\theta})$ is the likelihood of degradation observations under the estimation of model parameters $\hat{\theta}$. Based on the value of AIC, the one with the minimum AIC value is selected. On the other hand, the leave-out cross validation is to retain some degradation observation as validation observations. By calculating the errors of degradation inferences with these validation observations, the one with the minimum error is the best model. The procedure for this leave-out cross validation is demonstrated in the degradation analysis mentioned above to validate relevant degradation models.

In this paper, a comparison between the IG process models and the models based on the Wiener and gamma processes is studied using the leave-out cross validation method. The degradation observations of positioning accuracy are analyzed using the degradation models based on the Wiener and gamma processes. To model the S-shaped degradation rate, the degradation models based on the Wiener and gamma processes are separately formulated as follows.

- 1) Wiener process model for the degradation observations of positioning accuracy $\{Y^W(t), t \geq 0\}$:

$$\Delta y_{ij}^W(t_{ij}) \sim \text{Normal}(\Delta \Lambda_{ij}, \sigma^2 \Delta t_{ij}),$$

$$\Delta \Lambda_{ij} = \Lambda_{Si}(t_{ij}) - \Lambda_{Si}(t_{i,j-1}),$$

$$\Lambda_{Si}(t) = \nu_i \exp\left(\alpha \left(\frac{t}{\nu_i}\right) - \omega \left(\frac{t}{\nu_i}\right)^{-1}\right),$$

$$\nu_i \sim \text{Gamma}(\delta, \gamma). \quad (25)$$

- 2) Gamma process model for the degradation observations of positioning accuracy $\{Y^G(t), t \geq 0\}$:

$$\Delta y_{ij}^G(t_{ij}) \sim \text{Gamma}(\Delta \Lambda_{ij}, b),$$

$$\Delta \Lambda_{ij} = b(\Lambda_{Si}(t_{ij}) - \Lambda_{Si}(t_{i,j-1})),$$

$$\Lambda_{Si}(t) = \nu_i \exp\left(\alpha \left(\frac{t}{\nu_i}\right) - \omega \left(\frac{t}{\nu_i}\right)^{-1}\right),$$

$$\nu_i \sim \text{Gamma}(\delta, \gamma). \quad (26)$$

By implementing the proposed Bayesian framework for the degradation analysis using the Wiener process and gamma process models, the errors of degradation inferences under these models are obtained. A comparison of degradation inference errors among the Wiener process, gamma process, and IG process models is presented in Figs. 14 and 15. The IG process model is demonstrated to be more suitable for the degradation analysis of the machining accuracy than the Wiener process and gamma process models.

V. CONCLUSION

This study investigates the IG process models for the degradation analysis with constant, monotonic, and S-shaped degradation rates. An improved Bayesian framework for the degradation analysis with the IG process models is introduced as well. Degradation analysis of a heavy machining tool's spindle system is used to demonstrate the proposed methods step by step. These IG process models and the Bayesian framework have some promising features as follows. Time-varying degradation rates are introduced in the IG process models, where physical meaning of model parameters is highlighted. Other than monotonic and conditionally independent increments, these models have parametric degradation rates for their degradation processes. Failure mechanism and experts' testimony about the degradation processes can be incorporated through the degradation rates. The difficulties introduced by the situation of sparse degradation observations and the situation of evolving observations can then be solved by utilizing the parametric degradation rates and the extended Bayesian framework.

In addition, the IG process models with monotonic and S-shaped degradation rates have shape parameters and scale parameters, which are separately related to the shape of the degradation curve and the time scale of the degradation process. Prior information can be easily incorporated through these parameters under the Bayesian framework. Moreover, the

heterogeneities within product population can be handled through the incorporation of random effects on the scale parameters. In summary, these three IG process models and the proposed Bayesian framework jointly make the degradation analysis with parametric stochastic process models more flexible.

Other than the study presented above, there are some issues deserving further investigation. As the growth of parametric degradation process models, a comprehensive study about the model selection and comparison among these degradation models is urgent. Furthermore, application of the proposed IG process degradation models with the constructed Bayesian framework in accelerated degradation test, residual life prediction, and system health management is a valuable topic.

ACKNOWLEDGMENT

An earlier and much shorter version of this paper was presented at the Asia-Pacific International Symposium on Advanced Reliability and Maintenance Modeling 2014 (August 2014, Sapporo, Japan). Comments and suggestions from the reviewers and the Editor are very much appreciated.

REFERENCES

- [1] N. Chen and K. L. Tsui, "Condition monitoring and remaining useful life prediction using degradation signals: Revisited," *IIE Trans.*, vol. 45, no. 9, pp. 939–952, 2013.
- [2] X.-S. Si, W. Wang, C.-H. Hu, and D.-H. Zhou, "Remaining useful life estimation—A review on the statistical data driven approaches," *Eur. J. Oper. Res.*, vol. 213, no. 1, pp. 1–14, Aug. 2011.
- [3] Z.-S. Ye and M. Xie, "Stochastic modelling and analysis of degradation for highly reliable products," *Appl. Stoch. Models Bus. Ind.*, vol. 31, no. 1, pp. 16–32, 2015.
- [4] W. Peng, Y.-F. Li, Y.-J. Yang, J. Mi, and H.-Z. Huang, "Leveraging degradation testing and condition monitoring for field reliability analysis with time-varying operating missions," *IEEE Trans. Rel.*, vol. 64, no. 4, pp. 1367–1382, Dec. 2015.
- [5] M. Pecht and R. Jaai, "A prognostics and health management roadmap for information and electronics-rich systems," *Microelectron. Rel.*, vol. 50, no. 3, pp. 317–323, Mar. 2010.
- [6] C. J. Lu and W. Q. Meekeer, "Using degradation measures to estimate a time-to-failure distribution," *Technometrics*, vol. 35, no. 2, pp. 161–174, 1993.
- [7] D. Siegel, C. Ly, and J. Lee, "Methodology and framework for predicting helicopter rolling element bearing failure," *IEEE Trans. Rel.*, vol. 61, no. 4, pp. 846–857, Dec. 2012.
- [8] W. Wang, B. Hussin, and T. Jefferis, "A case study of condition based maintenance modelling based upon the oil analysis data of marine diesel engines using stochastic filtering," *Int. J. Prod. Econ.*, vol. 136, no. 1, pp. 84–92, 2012.
- [9] F. Zhao, Z. Tian, and Y. Zeng, "Uncertainty quantification in gear remaining useful life prediction through an integrated prognostics method," *IEEE Trans. Rel.*, vol. 62, no. 1, pp. 146–159, Mar. 2013.
- [10] H.-Z. Huang, H.-K. Wang, Y.-F. Li, L. Zhang, and Z. Liu, "Support vector machine based estimation of remaining useful life: Current research status and future trends," *J. Mech. Sci. Technol.*, vol. 29, no. 1, pp. 151–163, 2015.
- [11] S.-P. Zhu, Q. Lei, H.-Z. Huang, Y.-J. Yang, and W. Peng, "Mean stress effect correction in strain energy-based fatigue life prediction of metals," *Int. J. Damage Mech.*, 2016, to be published, doi: 10.1177/1056789516651920.
- [12] R. R. Zhou, N. Serban, and N. Gebrael, "Degradation modeling applied to residual lifetime prediction using functional data analysis," *Ann. Appl. Statist.*, vol. 5, no. 2B, pp. 1586–1610, 2011.
- [13] E. Abele, Y. Altintas, and C. Brecher, "Machine tool spindle units," *CIRP Ann. Manuf. Technol.*, vol. 59, no. 2, pp. 781–802, 2010.
- [14] R. Teti, K. Jemielniak, G. O'Donnell, and D. Dornfeld, "Advanced monitoring of machining operations," *CIRP Ann. Manuf. Technol.*, vol. 59, no. 2, pp. 717–739, 2010.
- [15] A. Verl, U. Heisel, M. Walther, and D. Maier, "Sensorless automated condition monitoring for the control of the predictive maintenance of machine tools," *CIRP Ann. Manuf. Technol.*, vol. 58, no. 1, pp. 375–378, 2009.
- [16] S. J. Bae, W. Kuo, and P. H. Kvam, "Degradation models and implied lifetime distributions," *Rel. Eng. Syst. Safety*, vol. 92, no. 5, pp. 601–608, May 2007.
- [17] J. I. Park and S. J. Bae, "Direct prediction methods on lifetime distribution of organic light-emitting diodes from accelerated degradation tests," *IEEE Trans. Rel.*, vol. 59, no. 1, pp. 74–90, Mar. 2010.
- [18] Z. Ye, L. C. Tang, and H.-Y. Xu, "A distribution-based systems reliability model under extreme shocks and natural degradation," *IEEE Trans. Rel.*, vol. 60, no. 1, pp. 246–256, Mar. 2011.
- [19] X. Liu and L. C. Tang, "A Bayesian optimal design for accelerated degradation tests," *Qual. Rel. Eng. Int.*, vol. 26, no. 8, pp. 863–875, Dec. 2010.
- [20] S. J. Bae and P. H. Kvam, "A nonlinear random-coefficients model for degradation testing," *Technometrics*, vol. 46, no. 4, pp. 460–469, 2004.
- [21] X. Liu, J. Li, K. N. Al-Khalifa, A. S. Hamouda, D. W. Coit, and E. A. Elsayed, "Condition-based maintenance for continuously monitored degrading systems with multiple failure modes," *IIE Trans.*, vol. 45, no. 4, pp. 422–435, 2013.
- [22] Z. Wang, H.-Z. Huang, Y. Li, and N.-C. Xiao, "An approach to reliability assessment under degradation and shock process," *IEEE Trans. Rel.*, vol. 60, no. 4, pp. 852–863, Dec. 2011.
- [23] J. Lawless and M. Crowder, "Covariates and random effects in a gamma process model with application to degradation and failure," *Lifetime Data Anal.*, vol. 10, no. 3, pp. 213–227, Sep. 2004.
- [24] C.-C. Tsai, S.-T. Tseng, and N. Balakrishnan, "Optimal design for degradation tests based on gamma processes with random effects," *IEEE Trans. Rel.*, vol. 61, no. 2, pp. 604–613, Jun. 2012.
- [25] Z. Pan and N. Balakrishnan, "Reliability modeling of degradation of products with multiple performance characteristics based on gamma processes," *Rel. Eng. Syst. Safety*, vol. 96, no. 8, pp. 949–957, Aug. 2011.
- [26] X.-S. Si, W. Wang, C.-H. Hu, M.-Y. Chen, and D.-H. Zhou, "A Wiener-process-based degradation model with a recursive filter algorithm for remaining useful life estimation," *Mech. Syst. Signal Process.*, vol. 35, nos. 1–2, pp. 219–237, Feb. 2013.
- [27] H. Liao and Z. Tian, "A framework for predicting the remaining useful life of a single unit under time-varying operating conditions," *IIE Trans.*, vol. 45, no. 9, pp. 964–980, 2013.
- [28] Z.-S. Ye, N. Chen, and Y. Shen, "A new class of Wiener process models for degradation analysis," *Rel. Eng. Syst. Safety*, vol. 139, pp. 58–67, 2015.
- [29] X. Wang and D. Xu, "An inverse Gaussian process model for degradation observations," *Technometrics*, vol. 52, no. 2, pp. 188–197, 2010.
- [30] S. Zhang, W. Zhou, and H. Qin, "Inverse Gaussian process-based corrosion growth model for energy pipelines considering the sizing error in inspection data," *Corros. Sci.*, vol. 73, pp. 309–320, Aug. 2013.
- [31] Z.-S. Ye and N. Chen, "The inverse Gaussian process as a degradation model," *Technometrics*, vol. 56, no. 3, pp. 302–311, 2014.
- [32] W. Peng, Y.-F. Li, Y.-J. Yang, H.-Z. Huang, and M. J. Zuo, "Inverse Gaussian process model for degradation analysis: A Bayesian perspective," *Rel. Eng. Syst. Safety*, vol. 130, pp. 175–189, Oct. 2014.
- [33] W. Peng, Y.-F. Li, Y.-J. Yang, S.-P. Zhu, and H.-Z. Huang, "Bivariate analysis of incomplete degradation observations based on inverse Gaussian processes and copulas," *IEEE Trans. Rel.*, vol. 65, no. 2, pp. 624–639, Jun. 2016.
- [34] D. N. P. Murthy, M. Xie, and R. Jiang, *Weibull Models*. Hoboken, NJ, USA: Wiley, 2004.
- [35] A. O'Hagan *et al.*, *Uncertain Judgements: Eliciting Experts' Probabilities*. Chichester, U.K.: Wiley, 2006.
- [36] T. Bedford, J. Quigley, and L. Walls, "Expert elicitation for reliable system design," *Statist. Sci.*, vol. 21, no. 4, pp. 428–450, 2006.
- [37] L. Walls and J. Quigley, "Building prior distributions to support Bayesian reliability growth modelling using expert judgement," *Rel. Eng. Syst. Safety*, vol. 74, no. 2, pp. 117–128, 2001.
- [38] I. S. Jawahira *et al.*, "Surface integrity in material removal processes: Recent advances," *CIRP Ann. Manuf. Technol.*, vol. 60, no. 2, pp. 603–626, 2011.
- [39] D. Lunn, D. Spiegelhalter, A. Thomas, and N. Best, "The BUGS project: Evolution, critique and future directions," *Statist. Med.*, vol. 28, no. 25, pp. 3049–3067, 2009.

Weiweng Peng received the Ph.D. degree in mechanical engineering from the University of Electronic Science and Technology of China, Chengdu, China, in 2015.

His research interests include degradation modeling, Bayesian reliability, and reliability analysis of complex systems.

Yan-Feng Li received the Ph.D. degree in mechatronics engineering from the University of Electronic Science and Technology of China, Chengdu, China, in 2013.

His research interests include reliability analysis and evaluation of complex systems and dynamic fault tree modeling.

Yuan-Jian Yang received the Ph.D. degree in mechanical engineering from the University of Electronic Science and Technology of China, Chengdu, China, in 2016.

His research interests include degradation modeling and reliability assessment.

Jinhua Mi is currently working toward the Ph.D. degree majored in mechanical engineering at the University of Electronic Science and Technology of China, Chengdu, China.

Her research interest is reliability analysis and evaluation of complex systems.

Hong-Zhong Huang (M'06) received the Ph.D. degree in reliability engineering from Shanghai Jiaotong University, Shanghai, China.

He is a Professor in the School of Mechanical, Electronic, and Industrial Engineering, University of Electronic Science and Technology of China, Chengdu, China. He has held visiting appointments at several universities in the USA, Canada, and Asia. He has published 200 journal papers and 5 books in the fields of reliability engineering, optimization design, fuzzy sets theory, and product development. His current research interests include system reliability analysis, warranty, maintenance planning and optimization, and computational intelligence in product design.

Dr. Huang is an ISEAM Fellow, a technical committee member of ESRA, a Co-Editor-in-Chief of the *International Journal of Reliability and Applications*, and an editorial board member of several international journals. He received the William A. J. Golomski Award from the Institute of Industrial Engineers in 2006, and the Best Paper Award of the ICFDM2008, ICMR2011, and QR2MSE2013.